

Proof of Innocence for the Quintessential Noninnocent Ligand TCNQ in Its Tetranuclear Complex with Four $[fac-Re(CO)_3(bpy)]^+$ Groups: Unusually Different Reactivity of the TCNX Ligands (TCNX = TCNE, TCNQ, TCNB)^{||}

Heiko Hartmann,[†] Wolfgang Kaim,^{*,†} Matthias Wanner,[†] Axel Klein,[†] Stéphanie Frantz,[†] Carole Duboc-Toia,[‡] Jan Fiedler,[§] and Stanislav Zális[§]

Institut für Anorganische Chemie, Universität Stuttgart, Pfaffenwaldring 55, D-70550 Stuttgart, Germany, Grenoble High Magnetic Field Laboratory, MPI-CNRS, 25, Avenue des Martyrs, BP 166, F-38042 Grenoble Cedex 9, France, and J. Heyrovský Institute of Physical Chemistry, Academy of Sciences of the Czech Republic, Dolejškova 3, CZ-18223 Prague, Czech Republic

Received March 3, 2003

The reactions of $[fac-Re(CO)_3(bpy)(MeOH)](PF_6)$, $bpy = 2,2'$ -bipyridine, with the TCNX ligands (TCNE = tetracyanoethene, TCNQ = 7,7,8,8-tetracyano-*p*-quinodimethane, and TCNB = 1,2,4,5-tetracyanobenzene) in CH_2Cl_2 gave very different results. No reaction was observed with TCNB whereas TCNE produced very labile intermediates which converted under mild conditions to structurally characterized $\{(\mu-CN)[fac-Re(CO)_3(bpy)]_2\}-(PF_6)$ with an eclipsed conformation relative to the almost linear Re–CN–Re axis (Re–N(NC) 2.134(8) Å, Re–C(CN) 2.098(8) Å). With TCNQ, a stable tetranuclear complex $\{(\mu_4-TCNQ)[Re(CO)_3(bpy)]_4\}(BF_4)_4$ was obtained. Its structural, electrochemical, and spectroscopic analysis indicates only negligible charge transfer from the rhenium(I) centers to the extremely strong π acceptor TCNQ. Evidence includes a calculated charge of only -0.09 for coordinated TCNQ according to the empirical structure/charge correlation of Kistenmacher, a high-energy nitrile stretching band $\nu_{CN} = 2235\text{ cm}^{-1}$, and unprecedented large anodic shifts $>0.7\text{ V}$ of the reduction potentials. DFT calculations were used to confirm and explain the absence of electron delocalization from the electron-rich metals to the TCNQ acceptor bridge. Correspondingly, the X-band and high-frequency (285 GHz) EPR data ($g = 2.007$) as well as the IR and UV–vis–NIR spectroelectrochemical results (marginal ν_{CO} shifts, TCNQ^{•-} chromophore bands) support the almost exclusive confinement of the added electron in $\{(\mu_4-TCNQ)[Re(CO)_3(bpy)]_4\}^{3+}$ to the TCNQ bridge.

Introduction

The TCNE and TCNQ molecules (TCNE = tetracyanoethene, TCNQ = 7,7,8,8-tetracyano-*p*-quinodimethane) are among the least “innocent”¹ of ligands in coordination chemistry² due to their very low-lying π^* orbitals. “Noninnocent”

ligands can occur in at least two readily accessible oxidation states which may introduce ambiguity in oxidation state assignment unless the “correct” oxidation numbers for metal and ligand can be proven experimentally.^{1c} Typically, the easily reducible ($E_{1/2} \approx -0.25\text{ V vs [Fe(C}_3\text{H}_5)_2]^{+/0}$) TCNE and TCNQ form radical ions TCNX^{•-} or even dianions TCNX²⁻ in their reactions with metal complexes, leading to mono-, di-, tri-, or tetranuclear nitrile-bonded (σ) complexes, to π complexes with side-on coordination, or to corresponding ion pair compounds (TCNX^{•-})(⁺ML_{*n*}) without direct coordination.² The combination of radicals TCNX^{•-} in conjunction with paramagnetic metal centers has produced some of the most remarkable molecular magnetic materials³

* To whom correspondence should be addressed. E-mail: kaim@iac.uni-stuttgart.de.

[†] Universität Stuttgart.

[‡] Grenoble High Magnetic Field Laboratory.

[§] J. Heyrovsky Institute of Physical Chemistry.

^{||} Dedicated to Hans Bock on the occasion of his 75th birthday.

(1) (a) Jørgensen, C. K. *Oxidation Numbers and Oxidation States*; Springer: Berlin, 1969. (b) Ward, M. D.; McCleverty, J. A. *J. Chem. Soc., Dalton Trans.* **2002**, 275. (c) Herebian, D.; Bothe, E.; Bill, E.; Weyhermüller, T.; Wieghardt, K. *J. Am. Chem. Soc.* **2001**, *123*, 10012.

(2) Kaim, W.; Moscherosch, M. *Coord. Chem. Rev.* **1994**, *129*, 157.

such as ferro-/ferrimagnetic (TCNE^{•-})[Fe(C₅Me₅)₂]^{4a} or (TCNE^{•-})₂V·0.5(CH₂Cl₂).^{4b,c} In addition, TCNQ-based materials, including organometallic species, were used for conduction studies.⁵

In combination with rhenium complexes, tri- and tetranuclear σ -bonded species $\{(\mu_3\text{-TCNQ})[\text{Re}(\text{CO})_5]_3\}(\text{BF}_4)_3$,⁶ $(\mu\text{-TCNQ})[\text{Re}_2\text{Cl}_4(\text{dppm})_2]_2$,⁷ and $(\mu_4\text{-TCNQ})[\text{Re}(\text{CO})_4\text{Cl}]_4$ ⁸ had been reported before we recently presented the first crystal structure of a discrete⁹ complex of 4-fold bridging TCNQ, $\{(\mu_4, \eta^1: \eta^1: \eta^1: \eta^1\text{-TCNQ})[\text{Re}(\text{CO})_3(\text{bpy})]_4\}(\text{BF}_4)_4$.¹⁰ Remarkably, the binding of four metal centers to already electron accepting TCNQ caused the complex to become even easier to reduce than the free ligand because of the apparent lack of π electron back flow from the metals to TCNQ. Herein we describe efforts to probe and understand this unexpected behavior in conjunction with synthetic attempts to obtain analogous complexes of TCNE and TCNB (TCNB = 1,2,4,5-tetracyanobenzene).¹¹

Whereas TCNB did not react at all with the $[\text{Re}(\text{CO})_3(\text{bpy})]^+$ fragment, the reaction with TCNE produced only labile species which were found to convert to the dinuclear cyanide bridged ion $\{(\mu\text{-CN})[\text{Re}(\text{CO})_3(\text{bpy})]_2\}^+$. That species had been obtained before by a conventional route,¹² its remarkable structure in the solid is reported here for the first time.

Experimental Section

Instrumentation. EPR spectra were recorded in the X-band on a Bruker System ESP 300 equipped with a Bruker ER035M

gaussmeter and a HP 5350B microwave counter. High-frequency EPR spectroscopy at 285 GHz was performed using a multifrequency spectrometer at 5 K.¹³ Gunn diodes operating at 95 and 115 GHz and equipped with a second and third harmonic generator have been used as a radiation source. An InSb bolometer (QMC Instruments) was used for detection. The main magnetic field was provided by a superconducting magnet (Cryogenics Consultant) which generates fields up to 12 T. Owing to different field sweep conditions, the absolute values of the g components were obtained by calibrating the precisely measured g anisotropy data with the isotropic g value from X-band measurements. While this procedure does not account for the temperature dependence of g , the values extracted are identical to those obtained using an added standard. The setup did not allow a completely air-free sample transfer. ¹H NMR spectra were taken on a Bruker AC 250 spectrometer, and infrared spectra were obtained using a Perkin-Elmer FTIR 1760X instrument. UV–vis–NIR absorption spectra were recorded on J&M TIDAS and Bruins Instruments Omega 10 spectrophotometers. Cyclic voltammetry was carried out in 0.1 M Bu₄NPF₆ solutions using a three-electrode configuration (glassy carbon electrode, Pt counter electrode, Ag/AgCl reference) and a PAR 273 potentiostat and function generator. The ferrocene/ferrocenium couple served as internal reference. Spectroelectrochemical measurements were performed using an optically transparent thin-layer electrode (OTTLE) cell¹⁴ for UV–vis and IR absorption spectra and a two-electrode capillary for EPR studies.¹⁵

Syntheses. The preparation and basic characterization of $\{(\mu_4\text{-TCNQ})[\text{Re}(\text{CO})_3(\text{bpy})]_4\}(\text{BF}_4)_4$ have been reported.¹⁰

$\{(\mu\text{-CN})[\text{Re}(\text{CO})_3(\text{bpy})]_2\}(\text{PF}_6)$ via TCNE Complex Intermediates. A mixture of 100 mg (0.217 mmol) of $\text{Re}(\text{CO})_3(\text{bpy})\text{Cl}^{16}$ and 55 mg (0.217 mmol) of AgPF₆ in 20 mL of CH₂Cl₂ and 5 mL of CH₃OH were reacted for 18 h. After removal of AgCl via filtration over Celite, the solvent was removed and replaced by 20 mL of pure CH₂Cl₂. To this yellow solution was added 7.0 mg (0.055 mmol) of TCNE, dissolved in 10 mL of CH₂Cl₂, upon which the color changed to blue-purple ($\lambda_{\text{max}} = 590$ nm; $\nu_{\text{CN}} = 2178$ w, $\nu_{\text{CO}} = 2038$ s, 1960 sh, 1934 s (in cm⁻¹)). Despite rapid removal of the solvent, the solid compound disintegrated rapidly within about 5 h at room temperature or within a week at -60 °C to the reddish-brown cyano-bridged dinuclear complex (28 mg, 50%) which was identified via IR and UV–vis absorption spectroscopy¹² and through a crystal structure analysis of the bis(dichloromethane) solvate (cf. below).

The cyano-bridged complex was also obtained from the reaction of $[\text{Re}(\text{CO})_3(\text{bpy})(\text{MeOH})](\text{PF}_6)$ with TCNE in a 1:1 molar ratio. Here, the TCNE complex intermediate had $\lambda_{\text{max}} = 494$ nm, $\nu_{\text{CN}} = 2177$ w, and $\nu_{\text{CO}} = 2038$ s, 1935 s, br (in cm⁻¹). In each case, the conversion from the TCNE complex intermediate to the cyanide-bridged dimer was more rapid in solution.

Analogous reactions of $[\text{Re}(\text{CO})_3(\text{bpy})(\text{MeOH})](\text{PF}_6)$ with TCNB in 1:1 or 4:1 molar ratios did not show any conversion even after one week of reaction time at room temperature.

Crystallography. Needle-shaped single crystals of $\{(\mu\text{-CN})[\text{Re}(\text{CO})_3(\text{bpy})]_2\}(\text{PF}_6) \cdot 2\text{CH}_2\text{Cl}_2$ were obtained from a saturated solution at -30 °C. Data were collected for an orange-brown specimen of the dimensions 0.4 × 0.15 × 0.08 mm³ using a Siemens P3 diffractometer. The structure was solved using direct methods with

- (3) (a) Miller, J. S.; Epstein, A. J. *Angew. Chem.* **1994**, *106*, 399; *Angew. Chem., Int. Ed. Engl.* **1994**, *33*, 385. (b) Miller, J. S.; Epstein, A. J. *Chem. Eng. News* **1995**, *73*, 30. (c) Miller, J. S.; Epstein, A. J. *Chem. Ind.* **1996**, 49. (d) Miller, J. S. *Interface* **2002**, *11*, 22.
- (4) (a) Yee, G. T.; Manriquez, J. M.; Dixon, D. A.; McLean, R. S.; Groski, D. M.; Flippen, R. B.; Narayan, K. S.; Epstein, A. J.; Miller, J. S. *Adv. Mater.* **1991**, *3*, 309. (b) Manriquez, J. M.; Yee, G. T.; McLean, R. S.; Epstein, A. J.; Miller, J. S. *Science* **1991**, *252*, 1415. (c) Pokhodnya, K. I.; Epstein, A. J.; Miller, J. S. *Adv. Mater.* **2000**, *12*, 410.
- (5) Fortin, D.; Drouin, M.; Harvey, P. D. *Inorg. Chem.* **2000**, *39*, 2758 and references cited.
- (6) Sacher, W.; Nagel, U.; Beck, W. *Chem. Ber.* **1987**, *120*, 895.
- (7) Bartley, S. L.; Dunbar, K. R. *Angew. Chem.* **1991**, *103*, 447; *Angew. Chem., Int. Ed. Engl.* **1991**, *30*, 448.
- (8) Leirer, M.; Knör, G.; Vogler, A. *Inorg. Chem. Commun.* **1999**, *2*, 110.
- (9) (a) Coordination polymers of μ_4 -TCNQ: (a) Shields, L. *J. Chem. Soc., Faraday Trans. 2* **1985**, *81*, 1. (b) O'Kane, S. A.; Clérac, R.; Zhao, H.; Ouyang, X.; Galán-Mascarós, J. R.; Heintz, R.; Dunbar, K. R. *J. Solid State Chem.* **2000**, *152*, 159. (c) Campana, C.; Dunbar, K. R.; Ouyang, X. *Chem. Commun.* **1996**, 2427. (d) Miyasaka, H.; Campos-Fernández, C. S.; Clérac, R.; Dunbar, K. R. *Angew. Chem.* **2000**, *112*, 3989; *Angew. Chem., Int. Ed. Engl.* **2000**, *39*, 3831. (e) Heintz, R. A.; Zhao, H.; Ouyang, X.; Grandinetti, G.; Cowen, J.; Dunbar, K. R. *Inorg. Chem.* **1999**, *38*, 144. (f) For a μ_4 -TCNE example see: Cotton, F. A.; Kim, Y. *J. Am. Chem. Soc.* **1993**, *115*, 8511.
- (10) Hartmann, H.; Kaim, W.; Hartenbach, I.; Schleid, T.; Wanner, M.; Fiedler, J. *Angew. Chem.* **2001**, *113*, 2927; *Angew. Chem., Int. Ed.* **2001**, *40*, 2842.
- (11) Discrete complexes of μ_4 -TCNX ligands: (a) Gross, R.; Kaim, W. *Angew. Chem.* **1987**, *99*, 257; *Angew. Chem., Int. Ed. Engl.* **1987**, *26*, 251. (b) Moscherosch, M.; Waldhör, E.; Binder, H.; Kaim, W.; Fiedler, J. *Inorg. Chem.* **1995**, *34*, 4326. (c) Waldhör, E.; Kaim, W.; Lawson, M.; Jordanov, J. *Inorg. Chem.* **1997**, *36*, 3248. (d) Baumann, F.; Kaim, W.; Olabe, J. A.; Párisse, A.; Jordanov, J. *J. Chem. Soc., Dalton Trans.* **1997**, 4455. (e) Diaz, C.; Arancibia, A. *Polyhedron* **2000**, *19*, 137. (f) Berger, S.; Hartmann, H.; Wanner, M.; Fiedler, J.; Kaim, W. *Inorg. Chim. Acta* **2001**, *314*, 22.
- (12) Kalyanasundaram, K.; Grätzel, M.; Nazeeruddin, Md. K. *Inorg. Chem.* **1992**, *31*, 5243.

(13) Barra, A.-L.; Brunel, L.-C.; Robert, J.-B. *Chem. Phys. Lett.* **1990**, *165*, 107.

(14) Krejčík, M.; Daněk, M.; Hartl, F. *J. Electroanal. Chem.* **1991**, *317*, 179.

(15) Kaim, W.; Ernst, S.; Kasack, V. *J. Am. Chem. Soc.* **1990**, *112*, 173.

(16) Abel, E. W.; Wilkinson, G. *J. Chem. Soc.* **1959**, 1501.

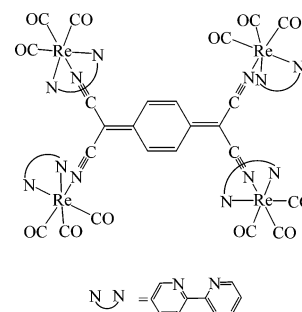
refinement by full-matrix least-squares of F^2 , employing the program package SHELXTL¹⁷ and the program X-SHAPE¹⁸ for absorption correction. All atoms other than hydrogen were refined anisotropically; hydrogen atoms were introduced using appropriate riding models.

DFT Calculations. Ground state electronic structure calculations of $\{(\mu_4\text{-TCNQ})[\text{Re}(\text{CO})_3(\text{bpy})]_4\}^{4+}$ complexes were performed on the basis of density-functional theory (DFT) methods using the ADF2000.2 program package.¹⁹ Within the ADF program, Slater type orbital (STO) basis sets of triple- ζ quality for Re and double- ζ quality for the remaining atoms were employed with polarization functions. The inner shells were represented by the frozen core approximation (1s for C, N, and O, 1s–4d for Re were kept frozen). The following density functionals were used within ADF: the local density approximation (LDA) with VWN parametrization of electron gas data or the functional including Becke's gradient correction²⁰ to the local exchange expression in conjunction with Perdew's gradient correction²¹ to LDA correlation (ADF/BP). The scalar relativistic (SR) zero-order regular approximation (ZORA) was used within this study.

Results and Discussion

Synthesis. Considering the typically similar reactivity of the TCNX ligands toward various complex fragments^{2,11} the reactions of these ligands with $[\text{fac-Re}(\text{CO})_3(\text{bpy})(\text{MeOH})](\text{PF}_6)$ in dichloromethane gave unexpectedly different results. (1) There was no reaction observed with TCNB even after one week as concluded from the absence of any change in color or IR spectroscopic response. (2) TCNE reacted via deeply colored labile intermediates (assumed to be complexes with intact TCNE) to a stable product which turned out to be the previously reported¹² but hitherto structurally uncharacterized $\{(\mu\text{-CN})[\text{Re}(\text{CO})_3(\text{bpy})]_2\}^+$ ion. We could now obtain single crystals of the hexafluorophosphate in solvated form for crystallographic structure determination (cf. below). The production of cyanide from TCNE has been described before as a result of TCNE $^{\bullet-}$ radical anion formation;^{22a,b} however, these reactions were reported to take place under more drastic conditions than the efficient conversion reported here which occurs both in solution and in the solid, at different metal to TCNE ratios, and even at low temperatures. Interestingly, photoinduced cyanide complex formation has been reported for $[\text{fac-(4-CNpy)Re}(\text{CO})_3(\text{bpy})]^+$, 4-CNpy = 4-cyanopyridine,^{22c} which points to a particular propensity of the $[\text{fac-Re}(\text{CO})_3(\text{bpy})]^+$ fragment for cyanide abstraction. Possibly metal-to-ligand charge-transfer excited states $[\text{Re}^{\text{II}}(\text{TCNE}^{\bullet-})]^*$ are also responsible here for the formation of $\{(\mu\text{-CN})[\text{Re}(\text{CO})_3(\text{bpy})]_2\}^+$; hexacyanobutadiene as a conceivable dimerization product from tricyanovinyl^{22a,b} was not isolated from the reaction mixture. (3) With TCNQ a

Scheme 1



stable tetranuclear complex (Scheme 1) was obtained from the reaction between the components at 4:1 molar ratio at room temperature. Its full characterization will be described in detail below. A trinuclear complex $\{(\mu_3\text{-TCNQ})[\text{Re}(\text{CO})_5]_3\}(\text{BF}_4)_3$,⁶ poorly soluble $(\mu_4\text{-TCNQ})[\text{Re}(\text{CO})_4\text{Cl}]_4$,⁸ and tetranuclear $(\mu\text{-TCNQ})[\text{Re}_2\text{Cl}_4(\text{dppm})_2]_2$ with triply bonded dirhenium(II) units⁷ have been reported; other complexes with 4-fold bridging TCNQ include discrete manganese,^{11a,c} ruthenium,^{11b} osmium,^{11d} iron,^{11e} and copper species^{11f} as well as polymeric systems with copper,^{9a,e} silver,^{9a,b} dimolybdenum,^{9c} dirhodium,^{9d} and diruthenium^{9d} units. Whereas the polymeric systems have been characterized crystallographically, the compound $\{(\mu_4\text{-TCNQ})[\text{Re}(\text{CO})_3(\text{bpy})]_4\}(\text{BF}_4)_4$ ¹⁰ represents the first structurally defined discrete complex of $\mu_4\text{-TCNQ}$.

The very different reactivity and product stability may be attributed to the variable electronic and steric properties of the TCNX ligands. TCNB is a distinctly weaker π acceptor than TCNE or TCNQ,² the reduction potential being more negative by about 0.8 V. TCNB is also a comparatively rigid ligand which may contribute to the lack of reactivity toward $[\text{fac-Re}(\text{CO})_3(\text{bpy})(\text{MeOH})]^+$. TCNQ is a much better π acceptor than TCNB; it offers four nitrile binding sites at sufficiently large metal–metal distances of 8.0 and 9.8 Å^{11c} to accommodate even four rather bulky complex fragments such as $[\text{Re}(\text{CO})_3(\text{bpy})]^+$ (cf. below). Planar TCNE provides four nitrile binding sites with approximately 6.0 Å (“1,2-dinitrile” side) and 8.0 Å distances (“1,1-dinitrile” side),^{11c} the former apparently too close to tolerate a stable tetranuclear complex with $[\text{Re}(\text{CO})_3(\text{bpy})]^+$. It is remarkable, however, that even at 1:1 molar ratio the TCNE and $[\text{Re}(\text{CO})_3(\text{bpy})(\text{MeOH})]^+$ reactants form only a labile intermediate which converts rapidly to a dimer bridged by cyanide as a disintegration product of TCNE.

Molecular Structure of $\{(\mu\text{-CN})[\text{Re}(\text{CO})_3(\text{bpy})]_2\}^+$. The crystallographic data of the hexafluorophosphate–bis(dichloromethane) solvate are summarized in Table 1; Figure 1 contains essential geometrical parameters. The molecular structure is shown in Figures 1 and 2.

The two $[\text{fac-Re}(\text{CO})_3(\text{bpy})]^+$ complex fragments are bridged by cyanide²³ in an almost linear fashion with bond angles between 175° and 180° within the OC–Re–NC–Re–CO axis. At 1.146(10) Å, the N1–C1 distance is not unusual.²³ The alternative Re2–N1–C1–Re1 shown in Figure 1 gave slightly better R values ($R_1 = 0.0482$, wR_2

(23) Dunbar, K. R.; Heintz, R. A. *Prog. Inorg. Chem.* **1997**, *45*, 283.

(17) Sheldrick, G. M. *Program package SHELXTL*; Bruker Analytical X-ray Systems: Madison, WI, 1998.

(18) *Programm X-SHAPE, Version 1.06*; Fa. STOE & Cie GmbH: Darmstadt, Germany, 1999.

(19) Fonseca Guerra, C.; Snijders, J. G.; Te Velde, G.; Baerends, E. J. *Theor. Chim. Acta* **1998**, *99*, 391. (b) van Gisbergen, S. J. A.; Snijders, J. G.; Baerends, E. J. *Comput. Phys. Commun.* **1999**, *118*, 119.

(20) Becke, A. D. *Phys. Rev A* **1988**, *38*, 3098.

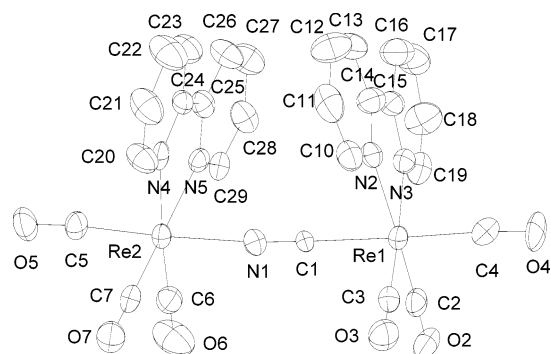
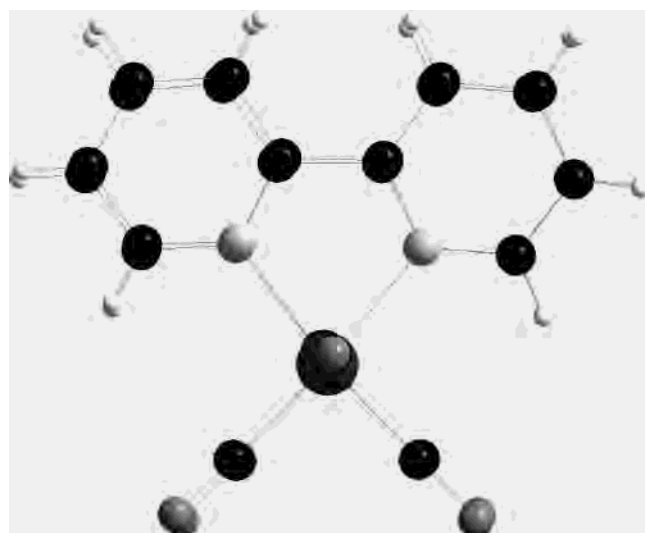
(21) Perdew, J. P. *Phys. Rev. A* **1986**, *33*, 8822.

(22) (a) Fatiadi, A. J. *Synthesis* **1986**, 249. (b) Fatiadi, A. J. *Synthesis* **1987**, 959. (c) Hori, H.; Ishihara, J.; Koike, K.; Takeuchi, K.; Ibusuki, T.; Ishitani, O. *Chem. Lett.* **1997**, 1249.

Table 1. Crystallographic Data of $\{(\mu\text{-CN})[\text{Re}(\text{CO})_3(\text{bpy})]_2\}(\text{PF}_6)_2 \cdot 2\text{CH}_2\text{Cl}_2$

chem formula	$\text{C}_{29}\text{H}_{20}\text{Cl}_4\text{F}_6\text{N}_5\text{O}_6\text{PRe}_2$
fw	1193.67
cryst syst, space group	monoclinic, $P2_1/n$ (No. 14)
T (K)	173(2)
a (Å)	11.382(4)
b (Å)	31.328(8)
c (Å)	11.865(4)
β (deg)	116.1(2)
V (Å ³)	3799(2)
Z	4
ρ_{calcd} in g cm^{-3}	2.087
μ (mm^{-1})	6.766
λ (Å)	0.71073
final R [$I > 2\sigma(I)$] ^a	$R_1 = 0.0482$
final R (all data) ^a	$R_w = 0.1076$

$$^a R_1 = (\sum ||F_o| - |F_c||) / \sum |F_o|. R_w = \{\sum [w(|F_o|^2 - |F_c|^2)^2] / \sum [w(F_o^2)^2]\}^{1/2}.$$

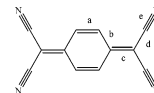

Figure 1. Molecular structure of the cation in the crystal of $\{(\mu\text{-CN})[\text{Re}(\text{CO})_3(\text{bpy})]_2\}(\text{PF}_6)_2 \cdot 2\text{CH}_2\text{Cl}_2$ with atom numbering (50% probability ellipsoids; hydrogen atoms are omitted for clarity): Re1–C1 2.098(8), Re2–N1 2.134(8), C1–N1 1.146(10), Re1–C2 1.882(9), Re1–C3 1.923(9), Re1–C4 1.962(10), Re2–C5 1.934(9), Re2–C6 1.902(9), Re2–C7 1.912(9), Re1–Re2 5.371(4), Re1–C1–N1 176.8(3), Re2–N1–C1 175.6(3), C4–Re1–C1 178.1(2), C5–Re2–N1 176.1(2).

Figure 2. Eclipsed conformation of $\{(\mu\text{-CN})[\text{Re}(\text{CO})_3(\text{bpy})]_2\}^+$ in the crystal.

$= 0.1076$) than Re2–C1–N1–Re1 ($R_1 = 0.0485$, $wR_2 = 0.1081$) or mixtures thereof which is an argument against CN disorder. The smaller Re–C distance relative to Re–N has been similarly observed for other cyanide complexes;²⁴ it is a consequence of the charge distribution in NC^- . The

Table 2. Intramolecular Bond Lengths (Å) (Scheme 2) in $\text{TCNQ}^{0/-25}$ and $\{(\mu_4\text{-TCNQ})\{\text{fac-Re}(\text{CO})_3(\text{bpy})\}_4\}(\text{PF}_6)_4$

compd	a	b	c	d	e	$b - c$	$c - d$	$c/(b + d)$
TCNQ	1.345	1.448	1.374	1.441	1.140	0.074	−0.067	0.476
TCNQ^{2-}	1.374	1.423	1.420	1.416	1.153	0.003	0.004	0.500
$[\text{Re}]_4\text{TCNQ}^a$	1.355	1.436	1.374	1.438	1.143	0.062	−0.064	0.478

^a Averaged values from ref 10.

Scheme 2


conformation as illustrated by the two perspectives in Figures 1 and 2 is quite remarkable: There is an almost complete eclipse along the Re–CN–Re axis (torsional angles $< 2^\circ$) with the bipyridine planes tilted toward each other (dihedral angle 22.2°). This apparent attraction between bpy π systems thus leads to a shortest interligand contact of 3.677(5) Å for the C12...C22 distance, a value which signifies weak π/π interaction.

Molecular Structure of $\{(\mu_4\text{-TCNQ})[\text{Re}(\text{CO})_3(\text{bpy})]_4\}^{4+}$.

The structure determination of the complex $\{(\mu_4\text{-TCNQ})[\text{Re}(\text{CO})_3(\text{bpy})]_4\}(\text{BF}_4)_4$ has been described.¹⁰ The isolated centrosymmetric tetracation contains an essentially planar $(\text{TCNQ})\text{Re}_4$ center with the bpy and CO co-ligands adopting two different conformations relative to that plane, probably to accommodate the four sterically demanding $[\text{Re}(\text{CO})_3(\text{bpy})]^+$ fragments. At 8.18 and 10.02 Å,¹⁰ the $\text{Re}\cdots\text{Re}$ distances are similar as estimated for such planar systems.^{11c} Despite the size of the molecule, the significant C–C distances of the TCNQ ligand were determined with sufficient accuracy to be used in the established approach^{9d,25} to determine the charge state of that ligand from the calculated and experimentally determined bond length variation. Table 2 summarizes these results which clearly indicate the unexpected¹¹ absence of any significant charge transfer in the ground state from the four rhenium(I) atoms to the TCNQ ligand.

A charge of $\rho = -0.09$ can be calculated for the TCNQ ligand from these bond parameters (see Scheme 2) and Kistenmacher's equation $\rho = -41.667 [c/(b + d)] + 19.833$,^{9d,25} confirming the $\mu_4\text{-TCNQ}^0$ assignment. The $\mu_4\text{-TCNQ}^0$ character is also confirmed by DFT calculations where a total Mulliken charge $\rho_M = -0.225$ is calculated for the TCNQ ligand.

Only a few metal compounds contain TCNQ in an essentially unreduced state,^{2,8,9d} among them one structurally characterized coordination polymer with $\mu_4\text{-TCNQ}^0$.^{9c} Much more common are metal compounds with TCNQ^{2-} in either isolated, dimerized, or coordinated form.² Thus, tetranuclear manganese,^{11ac} ruthenium,^{11b} osmium,^{11d} iron,^{11e} and copper^{11f}

(24) Calderazzo, F.; Mazzi, U.; Pampaloni, G.; Poli, R.; Tisato, F.; Zanazzi, P. F. *Gazz. Chim. Ital.* **1989**, *119*, 241. (b) Stark, G. A.; Arif, A. M.; Gladysz, J. A. *Organometallics* **1997**, *16*, 2909.

(25) (a) Kistenmacher, T. S.; Philips, J. E.; Cowan, D. O. *Acta Crystallogr., Sect. B* **1974**, *30*, 763. (b) Kistenmacher, T. S.; Emge, T. J.; Bloch, A. N.; Cowan, D. O. *Acta Crystallogr., Sect. B* **1982**, *38*, 1193. (c) Allen, D. P.; Bottomley, F.; Day, R. W.; Decken, A.; Sanchez, V.; Summers, D. A.; Thompson, R. C. *Organometallics* **2001**, *20*, 1840.

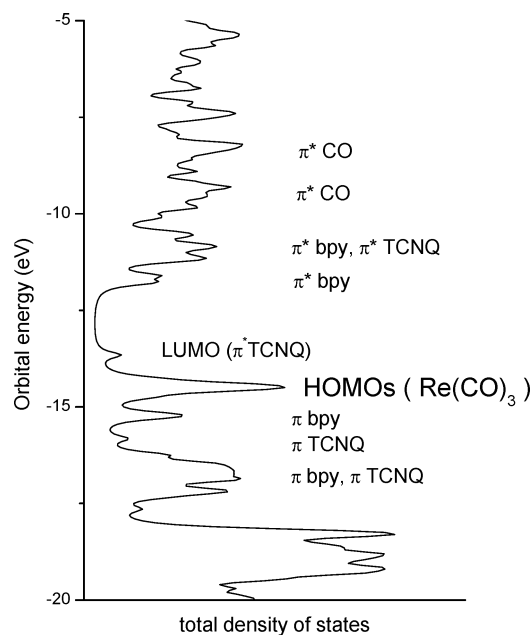


Figure 3. Molecular orbital diagram of $\{(\mu_4\text{-TCNQ})[\text{Re}(\text{CO})_3(\text{bpy})]_4\}^{4+}$ from DFT calculation as represented by the total density of states.

Table 3. ADF-Calculated One-Electron Energies and Percentage Composition of Selected MOs of $\{(\mu_4\text{-TCNQ})[\text{Re}(\text{bpy})(\text{CO})_3]_4\}^{4+}$ Expressed in Terms of Composing Fragments

MO	E (eV)	prevailing character	Re	CO	bpy	TCNQ
Unoccupied						
137a _u	-11.22	TCNQ + bpy			33	66
136a _u , 137a _g	-11.60					
135a _u , 136a _g	-11.78	bpy			99	
135a _g	-13.65	TCNQ + Re(CO) ₃	16	13	1	70
Occupied						
134a _u	-14.26	Re(CO) ₃ + TCNQ	53	33		13
133a _u , 134a _g	-14.41					
132a _u , 133a _g	-14.43					
131a _u , 132a _g	-14.50	Re(CO) ₃	58–60	36–39		1–3
130a _u , 131a _g	-14.51					
129a _u , 130a _g	-14.57					
129a _g	-14.75	Re(CO) ₃ + TCNQ	42	28		29
128a _u , 128a _g	-15.18					
127a _u , 127a _g	-15.27	bpy			99	
126a _u	-15.82	TCNQ	5	6	7	80

complexes of TCNQ were characterized as having a partially reduced central ligand by electrochemical and spectroscopic methods whereas the compound (TCNQ)[Re(CO)₄Cl]₄ contains neutral TCNQ, on the basis of high $\nu(\text{CN})$ values.⁸ Structural data for coordination polymers of $\mu_4\text{-TCNQ}$ involving dirhodium and diruthenium also suggested partial reduction, on the basis of bond length analysis.^{9d}

DFT Calculation Results for $\{(\mu_4\text{-TCNQ})[\text{Re}(\text{CO})_3(\text{bpy})]_4\}^{4+}$. The experimentally determined geometry of the tetracation in the crystal was used to calculate the electronic structure. The compositions of the frontier molecular orbitals are summarized in Table 3. Due to the size of the system with almost degenerate sets of 5d(Re), CO, and bpy orbitals in the frontier orbital region, a density-of-state versus energy representation was chosen (Figure 3).

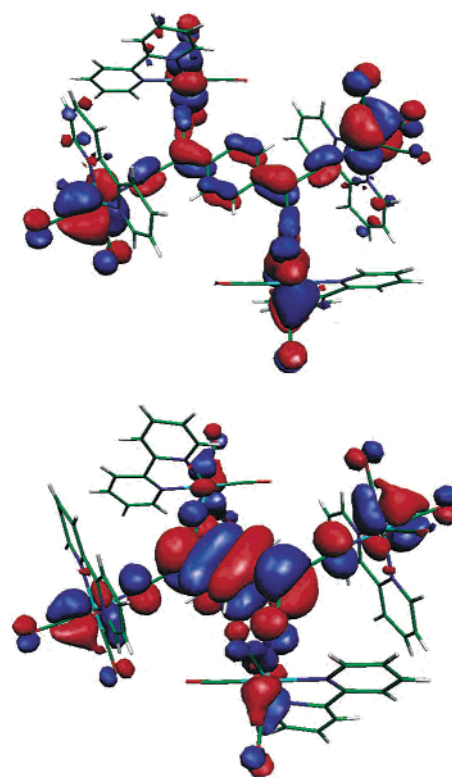


Figure 4. Molecular orbital representation of the HOMO (134a_u, top) and LUMO (135a_g, bottom) of $\{(\mu_4\text{-TCNQ})[\text{Re}(\text{CO})_3(\text{bpy})]_4\}^{4+}$ from DFT calculation.

The HOMO (134a_u) and LUMO (135a_g) are shown in Figure 4, illustrating the predominant contribution from the $\pi^*(\text{TCNQ})$ orbital for the latter whereas the HOMO is essentially a d_{Re} orbital combination.

Table 3 and Figure 3 show an unusually small HOMO/LUMO gap of 0.61 eV but a large LUMO/SLUMO separation of 1.87 eV, corresponding to the vast energy difference between the π^* orbitals of TCNQ and bpy (reduction potentials² of -0.25 and -2.55 V, respectively).

Spectroscopic Characterization of $\{(\mu_4\text{-TCNQ})[\text{Re}(\text{CO})_3(\text{bpy})]_4\}(\text{BF}_4)$. The tetranuclear complex exhibits a ¹H NMR spectrum with little shifted signals relative to those of the free ligands TCNQ and bpy or to those of other complexes of $\mu_4\text{-TCNQ}$ (Table 4).^{10,11}

The absence of broadened NMR lines is in agreement with the structure data, indicating essentially no electron and spin transfer to $\mu_4\text{-TCNQ}$. The equivalence of the four [*fac*-Re(CO)₃(bpy)]⁺ fragments in solution is also evident on the vibrational time scale where two intense carbonyl stretching bands (A, E) corresponding to the approximately trigonal local symmetry and one weak nitrile stretching band are observed (cf. Figure 6 and Table 6). Low intensity and broadness of the ν_{CN} band confirm the effective *D*_{2h} symmetry whereas the high wavenumber at 2235 cm⁻¹ in CH₂Cl₂, higher than for the free ligand (2227 cm⁻¹)²⁶ and most other tetranuclear complexes,¹¹ supports the notion of a practically unreduced TCNQ ligand. The tetraruthenium complex ($\mu_4\text{-TCNQ})[\text{Re}(\text{CO})_4\text{Cl}]_4$ has $\nu_{\text{CN}} = 2245$ and 2140 cm⁻¹ and

(26) Chappell, J. S.; Bloch, A. N.; Bryden, W. A.; Maxfield, M.; Poehler, T. O.; Cowan, D. O. *J. Am. Chem. Soc.* **1981**, *103*, 2442.

Table 4. Spectroscopic and Electrochemical Data of Complexes $(\mu_4\text{-TCNQ})[\text{ML}_n]_4$

$[\text{ML}_n]$:	$[\text{Re}(\text{CO})_3(\text{bpy})]^+$	$[\text{Mn}(\text{CO})_2(\text{C}_5\text{Me}_5)]$	$[\text{Os}(\text{CO})(\text{PR}_3)_2(\text{H})\text{Cl}]^a$	$[\text{Ru}(\text{NH}_3)_5]^{2+}$
δ_{CH} (ppm) ^b	7.32 (CD_2Cl_2)	¹ H NMR n.o. ^c	7.80 br (CD_2Cl_2)	7.70 ($(\text{CD}_3)_2\text{CO}$)
ν_{CN} (cm^{-1})	2235 (CH_2Cl_2)	IR 2170, 2105 (THF)	2180, 2140 (KBr)	2155, 2099 (CH_3CN)
λ_{max} (nm) [$\log \epsilon$ ($\text{M}^{-1} \text{cm}^{-1}$)]	680 [4.12], 382 [4.09] (CH_2Cl_2)	UV-vis-NIR 1418 [4.70] (toluene)	1170 [4.46], 697 [3.86] (DCE)	935 [4.70], 360 [4.04] (CH_3CN)
g_{iso}	2.0070 ^d	EPR n.o. ^c	2.0124 ^e (DCE)	2.019 (THF)
solvent	(CH_2Cl_2)	Electrochemistry ^f (DMF)	(CH_2Cl_2)	(CH_3CN)
E_{red1} (V)	+0.45	-0.58	-0.20	-0.59
E_{red2} (V)	+0.09	-0.80 ^g	-0.94	-0.84
K_c	$10^{6.1}$	$\approx 10^{3.2}$	$10^{12.5}$	$10^{4.2}$
ref	this work	11a,c	11d	11b

^a R = isopropyl. ^b $\delta_{\text{CH}}(\text{TCNQ})$, singlet. ^c Not observed due to metal-based paramagnetism (ref 11c). ^d In $\text{CH}_2\text{Cl}_2/\text{DCE}$ solution at 300K (X-band) and 5 K (285 GHz). ^e $g_{\perp} = 2.0160$, $g_{\parallel} = 2.0065$ at 110 K. ^f From cyclic voltammetry, 0.1 M Bu_4NPF_6 . $E_{1/2}$ values vs $\text{Fc}^{+/0}$. ^g Peak potential for irreversible reduction.

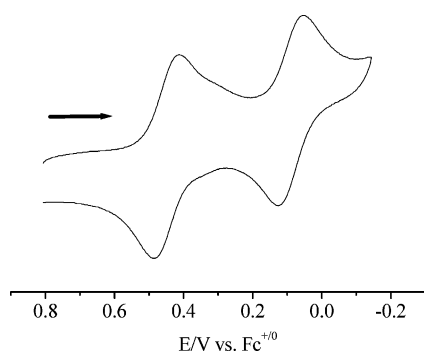


Figure 5. Cyclic voltammogram of $\{(\mu_4\text{-TCNQ})[\text{Re}(\text{CO})_3(\text{bpy})]_4\}(\text{PF}_6)_4$ in $\text{CH}_2\text{Cl}_2/0.1 \text{ M Bu}_4\text{NPF}_6$ at 100 mV/s scan rate, starting potential 0.8 V.

was described as containing neutral TCNQ as bridging ligand.⁸

Relatively high energy positions of $\nu_{\text{CO}} > 1910 \text{ cm}^{-1}$ have been similarly observed for dicationic complexes $[(\text{A})\text{Re}(\text{CO})_3(\text{bpy})]^{2+}$ with acceptor ligands A = 1-methylpyrazinium or 1-methyl-4,4'-bipyridinium (MQ^+).²⁷ Illustrations and data are given below in connection with spectroelectrochemical investigations.

The absorption spectrum of the tetranuclear TCNQ complex is dominated in the visible region by an intense broad band at $\lambda_{\text{max}} = 680 \text{ nm}$.¹⁰ Such long-wavelength bands, attributed to metal-to-ligand (MLCT)⁸ or ligand to-metal charge-transfer (LMCT) transitions, have also been observed for other tetranuclear complexes of TCNQ albeit at generally longer wavelengths in the near-infrared (NIR) region (Table 4). Since a high-energy transition would be expected for a small degree of mixing between well separated metal and ligand frontier orbitals we assign this band to an MLCT transition $d(\text{Re}^I) \rightarrow \pi^*(\text{TCNQ})$ similarly as in $(\mu_4\text{-TCNQ})\text{-}[\text{Re}(\text{CO})_4\text{Cl}]_4$ with $\lambda_{\text{max}} = 990$ and 700 nm .⁸ The band at 382 nm is identified as the slightly shifted TCNQ intraligand $\pi \rightarrow \pi^*$ transition; the $d(\text{Re}^I) \rightarrow \pi^*(\text{bpy})$ MLCT transitions are also expected to occur in that spectral region.

(27) Berger, S.; Klein, A.; Kaim, W.; Fiedler, J. *Inorg. Chem.* **1998**, *37*, 5664.

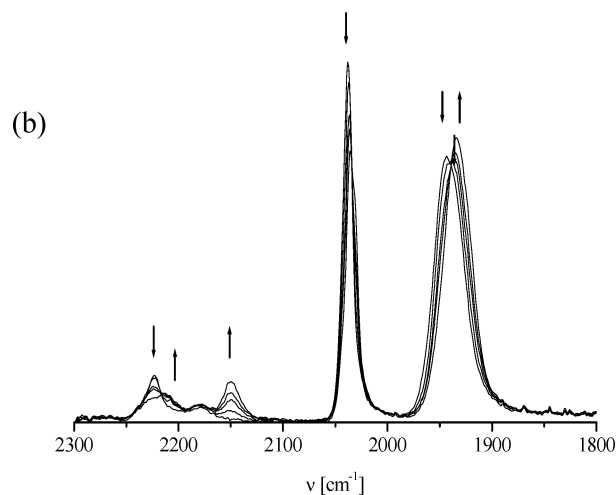
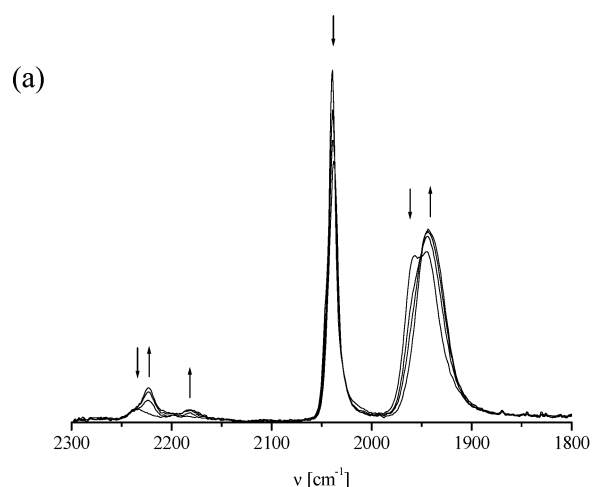


Figure 6. Changes of nitrile and carbonyl stretching bands on stepwise reduction of $\{(\mu_4\text{-TCNQ})[\text{Re}(\text{CO})_3(\text{bpy})]_4\}^{4+}$ from spectroelectrochemistry in $\text{CH}_2\text{Cl}_2/0.1 \text{ M Bu}_4\text{NPF}_6$: (a) transition (4+) \rightarrow (3+); (b) transition (3+) \rightarrow (2+).

Cyclic Voltammetry of $\{(\mu_4\text{-TCNQ})[\text{Re}(\text{CO})_3(\text{bpy})]_4\}\text{-}(\text{BF}_4)_4$. The tetranuclear complex exhibits an irreversible oxidation at a very high potential of +1.45 V versus $\text{Fc}^{+/0}$,

Table 5. UV–vis–NIR Data of $[(\mu_4\text{-TCNQ})\{\text{fac-Re}(\text{CO})_3(\text{bpy})\}_4]^{n+}$ from Spectroelectrochemistry in 0.1 M $\text{Bu}_4\text{NPF}_6/\text{CH}_2\text{Cl}_2$

<i>n</i>	λ_{max} (nm) [ϵ ($\text{M}^{-1} \text{cm}^{-1}$)]	tentative assignments
4	680 [13100]	MLCT (TCNQ)
	382 [12400]	IL (TCNQ),
	321 [26700]	MLCT (bpy)
3	1020 [16020]	IL (TCNQ $^{\bullet-}$)
	905 [11970]	IL (TCNQ $^{\bullet-}$)
	425sh	IL (TCNQ $^{\bullet-}$)
	405 [15620]	MLCT
2	320 [31400]	MLCT (bpy)
	925 [2970]	LMCT
	831 [2330]	LMCT
	425sh	MLCT (bpy)
	399sh	MLCT (bpy)
	341sh	MLCT (bpy)
	318 [46850]	IL

Table 6. IR Data of $[(\mu_4\text{-TCNQ})\{\text{fac-Re}(\text{CO})_3(\text{bpy})\}_4]^{n+}$ from Spectroelectrochemistry in 0.1 M $\text{Bu}_4\text{NPF}_6/\text{CH}_2\text{Cl}_2$

<i>n</i>	ν (cm^{-1})	
	ν_{CN}	ν_{CO}
4	2235w	2039vs, 1957s, 1945s
3	2223m, 2182w	2038vs, 1944s (br)
2	2210m, 2149m	2036s, 1939s (br)

presumably involving the rhenium(I) centers. Two reversible one-electron reduction processes at unusually high potentials (Table 4) are attributed to the TCNQ ligand (Figure 5): free TCNQ has $E_{\text{red1}} = -0.25$ V and $E_{\text{red2}} = -0.97$ V in $\text{CH}_3\text{CN}/0.1$ M Bu_4NPF_6 .^{2,11c}

For comparison, the bpy ligand reduction processes in related complexes $[(\text{A})\text{Re}(\text{CO})_3(\text{bpy})]^{2+}$, A = 1-methylpyrazinium or 1-methyl-4,4'-bipyridinium (MQ^+), lie at -1.57 and -1.60 V, respectively.²⁷ The difference between the anodic peak potentials of the oxidation ($+1.45$ V) and of the first reduction ($+0.48$ V) is only 0.97 V. This value compares with the calculated HOMO–LUMO difference of 0.61 eV (Table 3).

The anodically shifted first reduction potential puts this rhenium complex at one extreme end of a series as illustrated by Table 4. Atypically, the σ polarization of the TCNQ ligand through four metal centers is not compensated or overcompensated by π back-donation from the electron-rich metals to that excellent π acceptor.¹¹ Thus, the TCNQ ligand exhibits an unprecedented “normal” behavior on metal coordination which, however, results in a remarkably positive reduction potential, 0.45 V more positive than the reduction potential of ferrocenium and 0.74 V more positive than that of the already highly reducible free ligand,² the excellent π acceptor TCNQ.²⁸ It is not unexpected, therefore, that some preparations contained small amounts of the one-electron reduced complex as evident from EPR spectroscopy.

An interesting value indicative of the degree of metal–ligand interaction is the difference between the first two reduction potentials and, by use of eq 1, the comproportionation constant K_c for the paramagnetic intermediate, “int”.

$$K_c = \frac{[\text{int}]^2}{[\text{red}][\text{ox}]} = 10^{\Delta E/59\text{mV}} \quad (\Delta E = E_1 - E_2) \quad (1)$$

The K_c value amounts to about 10^{10} for TCNQ $^{\bullet-}$ ¹⁰ but

changes significantly in the series of Table 4. Stronger mixing of ligand π^* and metal d_{π} orbitals appears to result in smaller K_c values.

UV–Vis–NIR and IR Spectroelectrochemistry of $\{(\mu_4\text{-TCNQ})[\text{Re}(\text{CO})_3(\text{bpy})]_4\}(\text{BF}_4)_4$. Using an optically transparent thin-layer electrolytic (OTTLE) cell,¹⁴ we investigated the two reversible transitions during stepwise one-electron reduction. On the first electron uptake, the typical signature bands of the TCNQ $^{\bullet-}$ chromophore²⁸ were observed in the absorption spectrum (Table 5),¹⁰ shifted slightly to longer wavelengths. Other one-electron reduced complexes of tetranucleating TCNQ showed similar such bands.^{11b,d} The second reduction produces other long-wavelength bands (Table 5) which are tentatively assigned to $\pi(\text{TCNQ}^{2-}) \rightarrow d(\text{Re})$ ligand-to-metal charge-transfer (LMCT) transitions because TCNQ $^{2-}$ itself has no absorption bands in the visible.²⁹

Infrared spectroscopy in the nitrile and metal carbonyl stretching regions shows a very small response of ν_{CO} (Figure 6, Table 6), in agreement with the predominant addition of the electrons to a TCNQ-centered MO (Figure 4). Similarly small effects, i.e., shifts of less than 10 cm^{-1} , were reported for the acceptor (A)-based reduction processes of complexes $[(\text{A})\text{Re}(\text{CO})_3(\text{bpy})]^{2+}$, A = 1-methylpyrazinium or 1-methyl-4,4'-bipyridinium (MQ^+).²⁷

The very weak, broad nitrile stretching band of the tetracation comprises two allowed transitions in D_{2h} symmetry;^{2,11} it splits and shifts to lower energies on successive reduction (Figure 6, Table 6). This behavior is consistent with a TCNQ-based reduction, as the comparison with discrete¹¹ and polymeric coordination compounds⁹ of $\mu_4\text{-TCNQ}^{n-}$ illustrates; ν_{CN} of noncoordinated TCNQ n is shifted from 2228 cm^{-1} ($n = 0$) via 2197 and 2166 cm^{-1} ($n = 1-$) to 2164 and 2096 cm^{-1} ($n = 2-$).^{2,11d} The somewhat less pronounced shift for the tetrarhenium complex can be explained by the heavy metal coordination to the vibrating nitrile functions.

EPR of $\{(\mu_4\text{-TCNQ})[\text{Re}(\text{CO})_3(\text{bpy})]_4\}^{3+}$ at 9.5 and 285 GHz. The radical intermediate of the two-step reversible reduction could be studied for in situ electrolyzed solutions in the fluid and glassy frozen states and for solid preparations containing some amount of that radical complex. Unfortunately, attempts to obtain a pure radical compound through the reaction of $[\text{Re}(\text{CO})_3(\text{bpy})(\text{MeOH})](\text{PF}_6)$ with $\text{Li}(\text{TCNQ}^{\bullet-})$ have failed.

No hyperfine structure could be detected for the broad signal at $g_{\text{iso}} = 2.007$ measured at X-band frequency in solution at room temperature. Given the peak-to-peak line width of 1.5 mT and the approximate ^1H and ^{14}N hyperfine splitting expected for a TCNQ $^{\bullet-}$ ligand,^{28,30} we can estimate the $^{185,187}\text{Re}$ hyperfine coupling ($I = 5/2$) at less than 0.2 mT. In view of the very large anisotropic hyperfine coupling

(28) (a) Melby, L. R.; Harder, R. J.; Hertler, W. R.; Mahler, W.; Besnon, R. E.; Mochel, W. E. *J. Am. Chem. Soc.* **1962**, *84*, 3374. (b) Schulz, A.; Kaim, W. *Chem. Ber.* **1991**, *124*, 129.

(29) Suchanski, M. R.; Van Duyne, R. P. *J. Am. Chem. Soc.* **1976**, *98*, 250.

(30) Bell, E. S.; Field, J. S.; Haines, R. I.; Moscherosch, M.; Matheis, W.; Kaim, W. *Inorg. Chem.* **1992**, *31*, 3269.

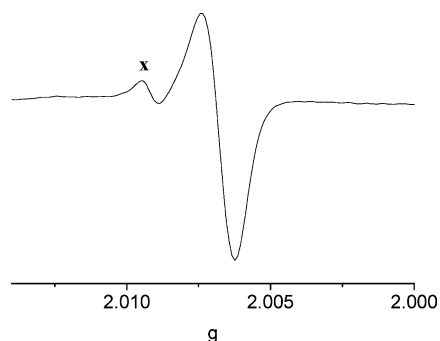


Figure 7. EPR spectrum of $\{(\mu_4\text{-TCNQ})[\text{Re}(\text{CO})_3(\text{bpy})]_4\}^{3+}$ at 285 GHz in $\text{CH}_2\text{Cl}_2/\text{DCE}$ (1/1) at 5 K (impurity signal x from sample transfer at $g = 2.009$).

parameters for the $^{185,187}\text{Re}$ isotopes,³¹ this indicates an only minute contribution from the metal centers to the singly occupied MO. Unusually small metal hyperfine splitting has also been observed for the complexes $[(\text{A})\text{Re}(\text{CO})_3(\text{bpy})]^{+}$ with $\text{A} = 1\text{-methylpyrazinium}$ or $1\text{-methyl-4,4'-bipyridinium}$ radicals.²⁷

The almost negligible effect of the four rhenium centers is also obvious from the just marginally³¹ shifted isotropic g value of 2.007 in comparison to 2.00265 for free $\text{TCNQ}^{\bullet-}$.³⁰ To establish the g tensor anisotropy, a better measure of the contributions from metals with high spin-orbit coupling constants,³¹ we investigated the radical complex ion $\{(\mu_4\text{-TCNQ})[\text{Re}(\text{CO})_3(\text{bpy})]_4\}^{3+}$ as present in a frozen $\text{CH}_2\text{Cl}_2/1,2\text{-dichloroethane}$ (1/1) solution of a partially reduced sample at 285 GHz in addition to the X-band study. However, even at that very high frequency, there was no g anisotropy detectable for the $g = 2.007$ signal (Figure 7), $\Delta g = g_1 - g_3$ is estimated at less than 0.001.

This result compares with the generally higher g_{iso} values and the detectable $\Delta g = 0.0095$ for tetra-ruthenium and -osmium complexes (Table 4). While the EPR results for the one-electron reduced tetra-rhenium(I) species are in qualitative agreement with the DFT calculated LUMO (Figure 4), the experimentally determined metal contribution is far lower than the calculated 16% (Table 3). In relation to complexes $\{(\mu\text{-L})[\text{Re}(\text{CO})_3(\text{X})]_2\}^{\bullet-}$, $\text{L} = \text{azopyridyl}$ ligands, which were studied by high-frequency EPR and analyzed with g -tensor calculations,³¹ the $\{(\mu_4\text{-TCNQ})[\text{Re}(\text{CO})_3(\text{bpy})]_4\}^{3+}$ ion displays far smaller hyperfine coupling and g anisotropy, suggesting combined metal contributions of less than 5% to the singly occupied MO.

Summary

Two results from this study are unexpected and remarkable, even considering the often extraordinary complexes

derived from the TCNX ligands.^{2-5,9,11} (1) There is an unprecedented variety in the reactivity of the $[\text{fac-Re}(\text{CO})_3(\text{bpy})(\text{MeOH})](\text{PF}_6)$ precursor with the three TCNX ligands used. The difference between high reactivity (TCNE) and nonreactivity (TCNB), between regular complex formation (TCNQ) and facile ligand disintegration (TCNE), must be attributed to the different combination of electronic and steric properties of these ligands. (2) The lack of any significant metal-to-ligand (TCNQ) electron transfer in the ground state of $\{(\mu_4\text{-TCNQ})[\text{Re}(\text{CO})_3(\text{bpy})]_4\}^{4+}$ is unequivocally demonstrated through the structural, electrochemical, and spectroscopic studies. While the DFT calculation confirms the narrow frontier MO gap, of this material it does not fully reproduce the observed virtual absence of metal contributions to the TCNQ-based LUMO. Obviously, the axial ligand L in $[\text{fac-Re}(\text{CO})_3(\text{bpy})(\text{L})]^+$ receives much less π electron density from the metal than bpy or similar chelate ligands, as observed before by example of mononuclear acceptor ($\text{L} = \text{A}$) complexes $[(\text{A})\text{Re}(\text{CO})_3(\text{bpy})]^{2+}$, $\text{A} = 1\text{-methylpyrazinium}$ or $1\text{-methyl-4,4'-bipyridinium}$ (MQ^+).²⁷ In turn, this allows for the special photochemistry³² and catalysis³³ involving that particular complex arrangement. As a consequence, the tetra-rhenium(I) complex $\{(\mu_4\text{-TCNQ})[\text{Re}(\text{CO})_3(\text{bpy})]_4\}^{4+}$ stands at the extreme end of a continuous series of compounds $(\mu_4\text{-TCNQ})[\text{ML}_n]$ (Table 4) with the metal-to-TCNQ electron transfer (and thus effective “noninnocence” of TCNQ) increasing along the sequence $[\text{ML}_n] = [\text{Re}(\text{CO})_3(\text{bpy})]^+ < [\text{Cu}(\text{Me}_3\text{TACN})]^+ < [\text{Os}(\text{CO})(\text{PR}_3)_2(\text{Cl})(\text{H})] < [\text{Mn}(\text{CO})_2(\text{C}_5\text{Me}_5)] < [\text{Ru}(\text{NH}_3)_5]^{2+}$.

Acknowledgment. This work was supported by COST D14 and D15 programs and by the “Access to Research Infrastructure Action of the Improving Human Potential Programme” of the European Union, by the Deutsche Forschungsgemeinschaft, the Volkswagenstiftung, and the Fonds der Chemischen Industrie. We also thank Dr. M. Niemeyer for crystallographic data collection.

Supporting Information Available: X-ray crystallographic file in CIF format for $\{(\mu\text{-CN})[\text{Re}(\text{CO})_3(\text{bpy})]_2\}(\text{PF}_6) \cdot 2\text{CH}_2\text{Cl}_2$ and table of bond parameters (Table S1). This material is available free of charge via the Internet at <http://pubs.acs.org>.

IC034232L

- (31) Frantz, S.; Hartmann, H.; Doslik, N.; Wanner, M.; Kaim, W.; Kümmerer, H.-J.; Denninger, G.; Barra, A.-L.; Duboc-Toia, C.; Fiedler, J.; Ciofini, I.; Urban, C.; Kaupp, M. *J. Am. Chem. Soc.* **2002**, *124*, 10563.
 (32) Summers, D. P.; Luong, J. C.; Wrighton, M. S. *J. Am. Chem. Soc.* **1981**, *103*, 5238.
 (33) Hawecker, J.; Lehn, J.-M.; Ziessel, R. *J. Helv. Chim. Acta* **1986**, *69*, 1990.